

## **Appendix 1**

# Self-Assembly Behavior Of Some Co- And Hetero-Polysaccharides Related To Hemicelluloses

Alan Esker<sup>1</sup>, Ulrike Becker<sup>2</sup>, Sylvie Jamin<sup>2</sup>,  
Shinji Beppu<sup>2</sup>, Scott Rennecker<sup>2</sup>, and Wolfgang Glasser<sup>2\*</sup>

<sup>1</sup>Department of Chemistry and <sup>2</sup>Department of Wood Science and Forest Products, Virginia Tech, Blacksburg, VA

The self-assembly behavior of a series of fluorinated cellulose ester copolymers with different F-substituents and with varying cellulose propionate (CP) molecular weight, and that of several xylan-rich hetero-polysaccharides and their derivatives, were examined in relation to their critical micelle concentration (CMC) and their interaction with model cellulosic surfaces. The F-containing CP derivatives had a telechelic architecture based on mono-functional CP segments of well-defined size; their F-content varied with the type of fluoro-alcohol group. The model cellulosic surface consisted of Langmuir-Blodgett films prepared from trimethylsilyl (TMS) cellulose in accordance with work by Schaub et al. Surface adsorption (“docking”) of water-soluble xylan derivatives was studied by surface plasmon resonance (SPR) spectroscopy. Surface deposition was also examined by atomic force microscopy (AFM). The results suggest that the CMC varies with both the chemical structure and the molecular weight of the amphiphile, and that cationic substituents and an enhanced hydrophilic/hydrophobic balance contribute to make the most strongly adsorbing water-soluble xylan on a cellulose surface. However, other xylylans also adhere to, or self-assemble on a model cellulosic surfaces. Several hypothetical aggregate structures are presented.

**Notice- This chapter appears in *Hemicelluloses: Science and Technology*, P. Gatenholm and M. Tenkanen, Eds., Symposium Series 864, pp. 198-219.**

**Copyright 2004 American Chemical Society.**

## Introduction

Self-assembly and self-organization are terms that describe the behavior of molecules as the purposeful response to environmental conditions. As such, self-assembly represents a form of smartness or intelligence (1,2). In the case of macromolecules, self-assembly behavior manifests itself in such spontaneous processes as the formation of aggregates in solution and the segregation of molecules at surfaces. Aggregation of copolymers occurs in solvents when one component is preferentially solvated over another component (3). This condition produces structures variably described as micelles, worm-like structures, lamellae, bi-layers, sheets, crew-cut micelles and vesicles (4,5). For AB di-block copolymers, the aggregation is usually limited to the formation of micelles similar to the ones observed in small-molecule surfactants (6). The micelles are formed by hiding the insoluble block in the core, thereby preventing precipitation.

We have previously synthesized a series of fluorine (F)-containing cellulose derivatives that have exhibited clear evidence of self-assembly in non-aqueous, organic solvent environments (7). The introduction of F-atoms into cellulose had originally been attempted with the aim of promoting compatibility between cellulose and synthetic polymers. The incorporation of fluorine into cellulose was accomplished by adding single F-atoms onto the backbone, or by covalently coupling F-containing substituents as grafts to the backbone (8-10).

F-containing cellulose derivatives are inherently amphiphilic molecules having a hydrophobic moiety (the F-substituent) covalently attached to a hydrophilic moiety (the cellulose backbone) (11). Similar amphiphiles on the basis of polysaccharides have been reported by Sunamoto et al. (12-15) and Uraki et al. (16, 17). Using water-soluble pullulan derivatized with cholesteryl substituents, Sunamoto et al. were able to study such features as the permeability of a polysaccharide-coated liposome as well as the fluidity of the liposomal membrane (12); the formation by self-aggregation of nanosize hydrogel particles in water (13); the complexation of an antitumor drug (adriamycin) in these hydrogel particles (14); and the macromolecular complexation of bovine serum albumin with these self-assembled nanoparticles (15).

Uraki et al., by contrast, was able to determine that the cellulose from unbleached organosolv pulp fibers (from acetic acid pulping), that is made water-soluble by hydroxypropylation, self-assembles into micellar structures on account of its inherent co-polymerization with (hydrophobic) lignin (16, 17). The amphiphilic hydroxypropyl cellulose-hydroxypropyl lignin copolymers of Uraki et al. are similar in architecture to isolated lignin-carbohydrate complexes, such as glucuronoxylans, that are associated with residual lignin fragments. Numerous studies have been dedicated to the nature

of this association in the past and, while there continues to be debate over the true nature of the bond (or bonds), there no longer is conflict over the fact that covalent bonds exist between the (hemicellulosic) carbohydrate portion and the lignin fraction (see other chapters in this book).

Fluorinated cellulose esters, cholesteroylated pullulan, lignin (derivative)-containing hydroxypropyl cellulose, and lignin-carbohydrate complexes (i.e., lignin-containing glucuronoxylan, or simply “xylan”, a widely represented hetero-polysaccharide in the plant kingdom) all have in common amphiphilic character and self-assembly behavior. Since only the first two types of molecules (i.e., the cellulose ester and the pullulan derivatives) are structurally designed by synthesis whereas the latter are subject to isolation from biocomposites that are frequently poorly described in structure and composition, an attempt is made in this study to define some molecular parameters important for self-assembly. This approach employs F-containing cellulose ester derivatives that (a) are “blocky” (or telechelic) in architecture, and (b) have variable molecular dimensions and substituent types.

Amphiphiles self-assemble differently in solution than at solid surfaces. The behavior of xylans at cellulosic surfaces (pulp fibers) has recently come under investigation by Henricksson and Gatenholm (19) who demonstrated that pulp fibers gain as much as 20% in weight when suspended in aqueous alkaline solutions of xylan at elevated temperature. Scanning electron microscopy (SEM) and atomic force microscopy (AFM) images revealed that the so-treated fibers contained particles (aggregates) within the cell wall structure of the fibers after treatment.

In order to achieve the overall goal of establishing the fundamental factors affecting adsorption to cellulose surfaces, two distinct steps are required. First, Langmuir Blodgett (LB) films (20) of regenerated cellulose are used to produce uniform surfaces that allow us to understand the physico-chemical underpinnings of adsorption without the morphological complications of a fiber surface. Second, the uniform cellulose layers, prepared on gold substrates, allow us to use surface plasmon resonance (SPR) experiments to monitor the adsorption of water-soluble polysaccharide derivatives onto the model cellulose surfaces.

Langmuir Blodgett (LB)-films of cellulose derivatives have been prepared in the past (21-25). Trimethylsilyl (TMS) cellulose dissolved in chloroform has been shown to form monolayers at the air-water interface (21). The layer has been shown to be transferrable onto solid hydrophobic surfaces. Multi-layered thin films of TMS cellulose can be easily desilylated using HCl vapors, producing a regenerated cellulose film with well-defined thicknesses and surface roughnesses. Such films have variably been used for studying self-assembly phenomena, immobilization tests of biomolecules (23), and determining surface energies of uncontaminated cellulose (21).

Surface plasmon resonance (SPR) is an optical technique that offers real time *in situ* analysis of dynamic events at solid surfaces and thus is capable of defining dimensional parameters of adsorbed mass, and rates of adsorption and desorption for a range of molecular interactions (26). While SPR has been widely utilized for biological applications, it is a relatively novel approach for studying adsorption in cellulosic systems. Hence, a brief description of the underlying principles and system requirements for SPR measurements is warranted. At the interface between a dielectric substance and metal, there exists a surface plasmon, a charge density that propagates longitudinally between the two media. For surface plasmons to exist at such an interface, the real parts of the dielectric constants of the two media must be of opposite sign. This condition is met in the near infrared (NIR) region for the air/metal and water/metal interfaces. At a critical angle, p-polarized laser light reflected at the interface of the two media interacts with the surface plasmon. A portion of the energy of the reflected light is coupled to the oscillating surface plasmon causing a decrease in intensity of the reflected light (parallel to absorption of energy in infrared spectroscopy). The critical angle will change as a function of the refractive index of the second medium, which is dependent on the thickness of the adsorbate. Gold is usually used as the metal coating on which the material to be studied is deposited. A schematic illustration of a typical SPR instrument can be found in Green et al. (26).

The objectives of the current study therefore dealt with exploring (a) the relationship between molecular parameters (block size and substituent type) and self-assembly behavior in F-containing cellulose esters (i.e., copolysaccharides), and (b) the self-assembly at solid surfaces (i.e., the “docking” behavior) of amphiphilic xylan molecules (i.e., heteropolysaccharides) at well-defined cellulose surfaces.

## Materials and Methods

### I. Materials:

Cellulose propionate was obtained from Eastman Chemical Company, Kingsport, TN. The mono-functional segments were synthesized in our laboratory as described previously (27, 28). Briefly, per-propionylated cellulose ester (CTP) was hydrolyzed with HBr in propionic anhydride and isolated by precipitation in water. The partially hydrolyzed CTP-oligomers were converted from the OH- to the NCO-terminated CTP derivatives by treatment with toluene diisocyanate (TDI) (27). The NCO-terminated, monofunctional segments were then reacted with various fluoro-alkyl alcohols to yield F-containing CTP telechelic copolymers. This procedure has been

employed previously for the purpose of studying surface segregation processes at cellulose ester surfaces (7).

Xylan was obtained from various biomass resources, including peanut hulls and rice husks, yellow poplar wood and rye straw using a method described previously (18). Cationic xylan was prepared by reacting xylan in aqueous alkali solution (pH 10 to 11) with glycidyl trimethyl ammonium chloride at 50°C for eight hours. The protocol followed work by Pulkkinen et al. with isolated lignin (29). The water-soluble reaction product was purified and isolated by membrane filtration and freeze-drying. It had an N-content of 2.30 wt.% corresponding to a DS of 0.3.

An anionic xylan derivative was produced by carboxymethylation of xylan in homogeneous 1N alkali solution using the sodium salt of chloroacetic acid, according to Gustavsson et al. (30). After 3 hr. at 70°C, the reaction mixture was adjusted to pH 10 with HCl and precipitated in ethanol.

A fluorine (F)-containing cationic xylan derivative was prepared by first reacting xylan in mildly alkaline aqueous solution with glycidyl-2, 2, 3, 3, 4, 4, 5, 5, 6, 6, 7, 7-dodeca-fluoroheptyl ether at 50° for two hours before further derivatizing the reaction product by the addition of additional alkali and the glycidyl trimethyl ammonium chloride reagent mentioned above. The reaction product was isolated, following neutralization and membrane filtration, by freeze-drying.

## II. Methods:

*Determination of critical micelle concentration (CMC) for cellulose ester derivatives:* The CMC was determined by measuring the surface free energy of low concentration-oligomer solutions. The F-containing cellulose ester derivatives were not cleanly soluble in any organic solvent, but formed turbid solutions in a variety of solvents, including acetone and THF. The xylan derivatives formed similarly turbid solutions in water. The two types of polysaccharide derivatives thereby exhibited both differences and similarities: they had vastly different solubility characteristics (organic solvent vs. water), and they formed colloidal solutions at low concentration on account of their bipolar structural characteristics. Cellulose esters were therefore measured in THF, and xylan derivatives were analyzed in water. For every oligomer or polymer, a 1% (w/v) solution in THF or water was made (stock solution), which was subsequently diluted as necessary. The surface free energy of the solutions were measured using a Cahn balance. A clean, round glass slide was connected to the beam of the balance, and the force was measured when the glass slide was lowered into the solution. Every measurement was carried out in triplicate. The value of the CMC was determined as percent (w/v) of oligomer or polymer in solution.

*Determination of critical micelle concentration (CMC) for xylan derivatives:* Surface tension measurements for the aqueous xylan solutions were made using the tensiometer from the Langmuir Blodgett trough system used below (KSV 2000). The surface tension was determined by the Wilhelmy plate technique using a sand blasted platinum plate. The xylan solutions were measured in a specially designed glass beaker that was cleaned with sulfuric acid. The temperature was held constant at 22.5°C by circulating thermostated water through the exterior of the beaker.

*Langmuir Blodgett (LB) film preparation:* The LB films of regenerated cellulose were prepared in accordance with an earlier publication by Schaub et al. (21). Trimethylsilyl (TMS) cellulose (Jena Biosciences, Ltd.) was used as chloroform-soluble derivative that was spread on the water surface of an LB-trough (KSV 2000) as a monomolecular film (20). A hydrophobic glass slide with a gold coating on one side was used as the SPR-suitable substrate for LB-film deposition.

*Adsorption (docking) experiments by surface plasmon resonance (SPR):* SPR-experiments were conducted on cellulose films prepared from a 40-layer film of TMS cellulose deposited by the LB method on glass slides coated with chromium and gold. The film on the glass side was removed with chloroform, and the film on the gold side was desilylated. The slide was then introduced into the SPR-apparatus. A refractive index matching oil was used to couple the back of the substrate to the SPR instrument. An oval plastic gasket was positioned on the slide, and the cell was placed on top. The cell was linked by two tubing lines to a pump. Both lines can be placed into the same solution to avoid pumping air during the transition to a second solution. The solutions used were prepared with distilled, deionized water. All solutions were prepared at concentrations of 10, 40, 100, 200, 1000, 2000, and 4000 mg L<sup>-1</sup>. The solutions were allowed to run in the cell until the signal indicated the establishment of near-equilibrium conditions. This situation usually required not more than a few minutes. Water was eluted for a few minutes before the line was switched to a solution of higher concentration. Adsorption due to this more concentrated solution thus occurred on top of the already adsorbed solids from the previous solution. This means that the solute present in the 10 mg L<sup>-1</sup>-solution adsorbed on a clean cellulose surface, but all other solutions were adsorbed on top of what had already been absorbed from the solution with the next lower concentration. The solutions were run through the cell on the gold slide at a flow rate of 0.45 mL min<sup>-1</sup>, and the changes in the resonant angle, which can be related to the thickness, were recorded every 10 s.

*Atomic Force Microscopy (AFM) image acquisition:* AFM measurements were conducted on films cast on mica slides. The films were coated with self-assembling substances by immersion in the respective solutions at room temperature and stored at 4 C. AFM measurements were conducted in tapping mode on a Digital Instruments Dimension 3000 Scope, with a Nanoscope IIIa

controller. Several samples using at least two different silicon nitride tips were used for each film in order to exclude artifacts.

## Results and Discussion

**Self-Assembly Measurements in Solution:** The critical micelle concentration (CMC) is the characteristic solution concentration at which solubilized single molecules aggregate into micellar structures. A number of parameters, including osmotic pressure, conductivity, turbidity and surface tension experience dramatic changes at the CMC. One method of determining the CMC involves surface tension measurements using a Wilhelmy plate. The CMC of various F-terminated cellulose ester oligomers and of xylans were determined in THF and water, respectively.

The F-terminated cellulose esters varied by size of the cellulose ester (cellulose propionate, CP) segment, which ranged between the degree of polymerization (DP) of 15 and 70; and it varied by type of F-containing end group, which was either a trifluoroethoxy, octafluoropentoxy, or perfluorooctanoxy end group (Table I and Figure 1). The xylan derivatives varied by substituent type and functionality: there was an *anionic* derivative, a *cationic* derivative, and an *F-containing cationic* derivative (Figure 2).

**Table I: Overview of block-like (telechelic) cellulose ester copolymers. (S. Figure 1 for structure).**

Sample designation	DP of CP Block <sup>a</sup>	End-group type	Number of F-atoms in substituent	F-content (%) <sup>b</sup>	CP mass per endgroup (g/mole) <sup>c</sup>
T <sub>15</sub> <sup>d</sup> -TF <sup>e</sup>	15	Trifluoro	3	0.87	4950
T <sub>15</sub> -PF	15	Perfluoro	13	3.63	4950
T <sub>15</sub> -OF	15	Octafluoro	8	2.29	4950
T <sub>30</sub> -TF	30	Trifluoro	3	0.45	9900
T <sub>30</sub> -PF	30	Perfluoro	13	1.91	9900
T <sub>30</sub> -OF	30	Octafluoro	8	1.19	9900
T <sub>70</sub> -TF	70	Trifluoro	3	0.18	23000
T <sub>70</sub> -PF	70	Perfluoro	13	0.78	23000
T <sub>70</sub> -OF	70	Octafluoro	8	0.48	23000

<sup>a</sup> Calculated from molecular weight data

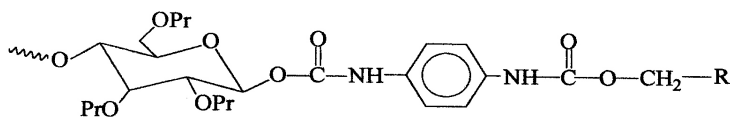
<sup>b</sup> Calculated as atomic % of F-atoms on all atoms of the sample, excluding protons

<sup>c</sup> Calculated from GPC data

<sup>d</sup> Indicates DP of CP-block

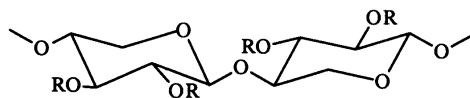
<sup>e</sup> Indicates type of end-group





where R = - CF<sub>3</sub> (trifluoro)  
 - CF<sub>2</sub>CF<sub>2</sub>CF<sub>2</sub>CF<sub>2</sub>H (octafluoro)  
 - CH<sub>2</sub>CF<sub>2</sub>CF<sub>2</sub>CF<sub>2</sub>CF<sub>2</sub>CF<sub>3</sub> (perfluoro)

Figure 1. Structural schemes of F-containing cellulose ester copolymers.



#### XYLAN DERIVATIVES

R = H and some lignin (10-15% by wt.), Xylan  
 R = -CH<sub>2</sub>-CH(OH)-CH<sub>2</sub>-N<sup>+</sup>(CH<sub>3</sub>)<sub>3</sub>Cl<sup>-</sup>, Cationic Xylan  
 R = -CH<sub>2</sub>-CO<sub>2</sub>H, Anionic Xylan  
 R = -CH<sub>2</sub>-CH(OH)-CH<sub>2</sub>-N<sup>+</sup>(CH<sub>3</sub>)<sub>3</sub>Cl<sup>-</sup>/  
 -CH<sub>2</sub>-CH(OH)-O-CH<sub>2</sub>-(CF<sub>2</sub>)<sub>6</sub>-H,  
 F-containing Cationic Xylan  
 F-containing Cationic Xylan

Figure 2. Structural schemes of water-soluble xylan derivatives used for adsorption studies on cellulosic LB-surfaces.

The presence of amphiphilic cellulose esters and xylan derivatives in THF and water, respectively, causes a decrease in the surface free energy for the solution as the surface-active molecules adsorb at the air/solution interface. By measuring the change in surface tension as a function of bulk solution concentration, it is possible to estimate the critical micelle concentration (CMC), the point where surfactant molecules self-assemble into larger aggregates. For small molecule surfactants, these aggregates possess well-defined sizes, shapes, and large aggregation numbers, the number of molecules needed to make the micelle. For polydisperse polymeric amphiphiles, the "micellar" sizes, shapes, and aggregation numbers, are more poorly defined. In general, polymeric species exhibit aggregation numbers that are typically

much smaller than regular small-molecule surfactants in accord with the closed-association model for micelle formation (31). As a consequence, the transitions seen in Figure 3, where "surface tension" is plotted as a function of bulk solution concentration are not as sharp as one might find for typical small molecule surfactants like sodium dodecylsulfate (31). In principle, the change in surface tension with respect to bulk solution concentration can also be used to obtain the surface concentration of the surfactant,  $\Gamma_2$ , through the Gibbs adsorption isotherm:

$$\Gamma_2 = -\frac{1}{RT} \left( \frac{\partial \gamma}{\partial \ln a_2} \right) \quad [1]$$

$$\lim_{c_2 \rightarrow 0} \Gamma_2 = -\frac{1}{RT} \left( \frac{\partial \gamma}{\partial \ln c_2} \right) \quad [2]$$

where  $\gamma$  is the surface tension of the solution,  $a_2$  is the activity of the solute,  $c_2$  is the concentration of the solute,  $R$  is the gas constant, and  $T$  is the temperature. Plotting the data in Figure 3 as a function of  $\log c_2$  would provide a slightly better interpretation of the data with respect to the estimation of the CMC, and calculation of  $\Gamma_2$ . However, the absence of activity data, the fact that we have polydisperse samples, and the lack of actual  $\gamma$  values for the CTP series of polymers, precludes such a detailed analysis.

Figure 3A, shows "wetting force" as a function of bulk solution concentration for T<sub>70</sub>-TF in THF. Here, "wetting force" is the mass of a round glass plate in contact with a CTP solution as measured by a Cahn balance. As the mass is proportional to the surface tension one gets in a true Wilhelmy plate method, Figure 3A is equivalent to a plot of  $\gamma$  vs.  $c_2$ . From the plot, it is clear that there is a transition from one-type of linear behavior at low concentration to a different linear regime at higher concentration. At low CTP concentrations,  $a_2 \cong c_2$  and  $\Gamma_2 \propto (\partial\gamma/\partial \ln c_2)$ . At higher concentrations,  $a_2 \approx$  a constant independent of  $c_2$  so  $(\partial\gamma/\partial \ln c_2)$  grossly distorts the fact that the chemical potential of the solute is not significantly changing with increasing solute concentration. Hence, the intersection of these two regimes provides a qualitative measure of the CMC. For the CTP series, two distinct trends (Figures 4 & 5) are noted:

- 1) the CMC depends on the type of F-end group used,  $CMC_{\text{octafluoro}} > CMC_{\text{trifluoro}} > CMC_{\text{perfluoro}}$ ; and
- 2) the CMC increases with the degree of polymerization.

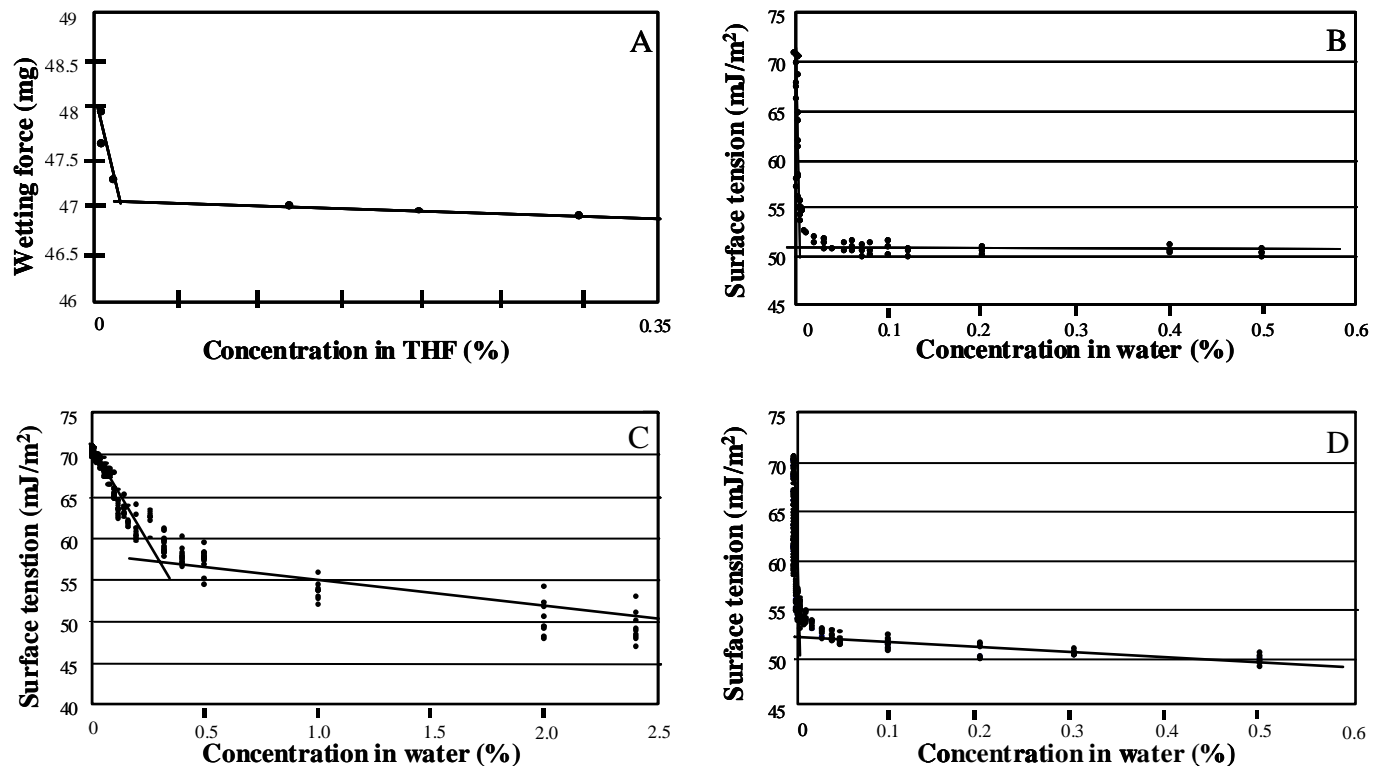


Figure 3. Illustration of critical micelle concentration (CMC) measurement results using the modified Wilhelmy plate method. CMC is obtained as the intercept of the linear portion of two slopes relating wetting force (or surface tension) to analyte concentration. (A) Typical blocky (telechelic) fluorinated cellulose ester copolymer ( $T_{70}$ -TF) (data are averages of three measurements with a variation of  $\pm 0.25$ ); (B) xylan from rye straw (data variation as shown); (C) xylan from yellow poplar; and (D) hydroxypropyl xylan derivative.

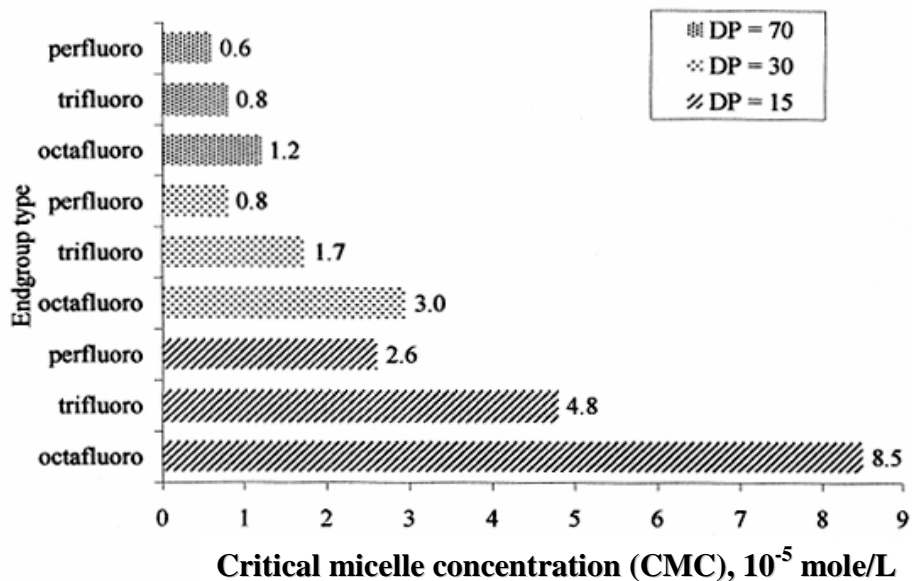


Figure 4. CMC values obtained with F-containing, telechelic cellulose ester copolymers having variable substituent type and variable cellulose ester-molecular size (expressed in DP).

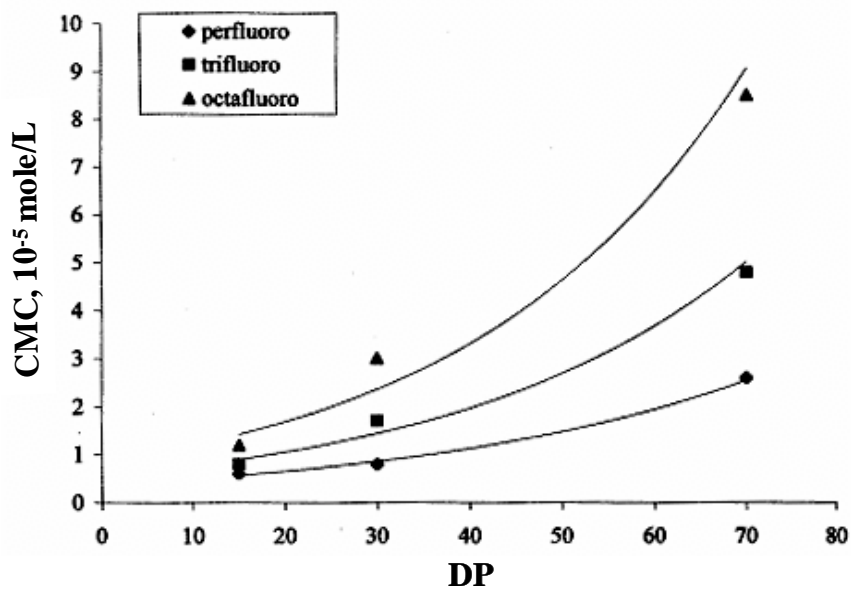


Figure 5. Dependence of CMC on the DP of the cellulose ester block for different F-containing end groups.

Both effects can be rationalized in terms of the balance between "hydrophobic" and "hydrophilic" interactions. As the CTP is more THF compatible than the fluorinated end groups, CTP represents the "hydrophilic" part of the molecule. Hence, as the molecular weight of CTP  $\uparrow$ , THF compatibility  $\uparrow$ , and a bigger CMC is observed in response to the increased "hydrophilic" character of the molecule. For the effect of fluorination, it is important to note that the F-endgroups represent the "hydrophobic" part of the molecule in THF. For trifluoro vs. "perfluoro" endgroups, it is clear that the "perfluoro" group is more "hydrophobic" than the fluorinated methyl end group, hence a lower CMC is expected and observed. However, one might also rationalize that the octafluoro end group should lie between the trifluoro and "perfluoro" derivative based solely on the number of F atoms. The reason that the CMC for the CTP with octafluoro end groups is actually bigger than CTP with trifluoro or "perfluoro" endgroups appears to be due to a strong dipole residing on the terminal C-H bond. The polarity of the C-H bond arises from the fact that strongly electronegative F substituents reside on the same carbon as well as on the adjacent carbon atoms. This strong dipole may allow the  $\text{CF}_2\text{-H}$  terminus to engage in secondary interactions that significantly enhance the polymer-solvent compatibility, thereby resulting in a larger CMC. This hypothesis is consistent with the observation that  $\omega$ -hydroxy functional quaternary ammonium bolaform surfactants have a significantly larger CMC than the corresponding non-hydroxylated surfactants (32). This difference was explained with the ability of the hydroxy-terminus to hydrogen bond with the solvent.

Even though the CTP polymers with fluorinated end groups were only soluble in THF, their ability to aggregate in solution offered insight into how one might change the structure of xylan-rich heteropolysaccharides, or simply "xylan" for short, to produce water-soluble amphiphilic molecules. To this end, a series of xylan-rich heteropolysaccharides and their more water-soluble hydroxypropyl (HP) and acetoxypropyl (AP) derivatives (33) were prepared. As these materials were water soluble, it was possible to easily measure the true surface tension of the aqueous solutions by the Wilhelmy plate method. Hence, Figures 3B-3D, show  $\gamma$  as a function of the bulk solution concentration. Overall, the xylan-rich heteropolysaccharides and their HP and AP derivatives exhibited a wide range of CMC values ( $0.01\text{-}5.0 \text{ g}\cdot\text{L}^{-1}$ ). However, these three plots are representative examples for two important trends:

1. Xylan obtained from different sources or isolation procedures exhibits extremely different CMC values (Figure 3B vs. 3C);
2. In general, HP or AP xylan derivatives (33), produced sharp transitions in surface tension with respect to bulk solution concentration and distinct CMC values (Figure 3D), whereas most (Figure 3D), but not all (Figure 3B), xylan isolated from natural

sources do not exhibit sharp changes in surface tension with changing bulk solution concentration and hence have less definitive CMC values.

Weak transitions, like the one in Figure 3C, are indicative of ill-defined aggregates in solution with small aggregation numbers. Nonetheless, the fact that xylans with different lignin-levels (Figure 3B) or chemical modification by HP or AP derivatives (Fig. 3D) could alter and sharpen the CMC provided encouragement that xylan-derivatives could be made that would adsorb ("dock") more strongly on a cellulose surface.

**Self-Assembly Measurements at Solid Surfaces:** Surface plasmon resonance (SPR) spectroscopy produces observations regarding the adsorption of solid (colloidal) mass at smooth surfaces from solution (26). LB films of regenerated cellulose represent multilayered architectures of cellulose molecules, with each layer having the thickness of a single cellulose molecule (4.2 Å) (34). These films and their structures have previously been described in the literature (21-26). The usual 40 to 60-layered films have an overall thickness of 15 to 20 nm, and they are totally clear and transparent. These films produce a contact angle with water of between 23 and 55° (21, 23).

SPR-experiments using the instrumental arrangement described by Green et al. (26) provide experimental observations related to film thickness (in pixel-values) on a time or concentration scale. Film thickness in pixels is determined by measuring the location of the baseline after correcting for changes in the bulk refractive index of the film due to changes induced by the solvent. Film thickness in pixels is related to a distance dimension according to a complicated relationship involving the response coefficient of the adsorbed substance, a reflection angle value, and many other parameters. Since the coefficient of the specific solutes have not been determined, no rigorous relationship can be established at this time. Nevertheless, an approximate thickness measure can be derived from the knowledge that each cellulose layer has a thickness of 4.2Å (34). By measuring the change in resonant angle in pixels for films with different numbers of cellulose layers (0, 10, 20, 40, and 60 layers), an approximate relationship between number of pixels and film thickness can be established. A conversion factor of 0.49 pixels/Å has been established experimentally.

Several water-soluble, xylan-rich hetero-polysaccharides and their derivatives were measured in this way with respect to their self-assembly behavior at cellulosic LB film surfaces (i.e., "docking" behavior). The corresponding experimental results are summarized in Figure 6. The structure of the xylan derivatives used is given in Figure 2.

Xylan itself is a hetero-polysaccharide that forms colloids at low solution concentration. Results indicate that a little xylan is adsorbed, slowly, at

concentrations above the CMC (Figure 6). By adding cyclodextrin to the xylan colloidal solution, xylan becomes more water soluble (as judged by the unaided eye), and the adsorption behavior as revealed by SPR changes (Figure 6). Very little xylan is adsorbed with the change in resonant angle leveling-off point at around 3 pixels. This value corresponds to a film  $\approx 1.5\text{\AA}$  thick. As this value is too small to be consistent with a homogeneous monolayer, the surface must be weakly populated by “micellar” aggregates. When cyclodextrin is present, the same adsorbed amount is reached at a lower bulk solution concentration and the maximum adsorption plateaus at a slightly higher value (Figure 6). Anionically-modified xylan (CMX) shows behavior similar to that of xylan with cyclodextrin: rapid adsorption to a submonolayer adsorbed film (Figure 6).

Based on the above results, it was clear that more drastic changes in xylan structure were required to promote adsorption (“docking”). Hence cationic and F-containing xylan derivatives were examined given the strong “hydrophobic” effect seen for F-containing CTP derivatives. Cationically-

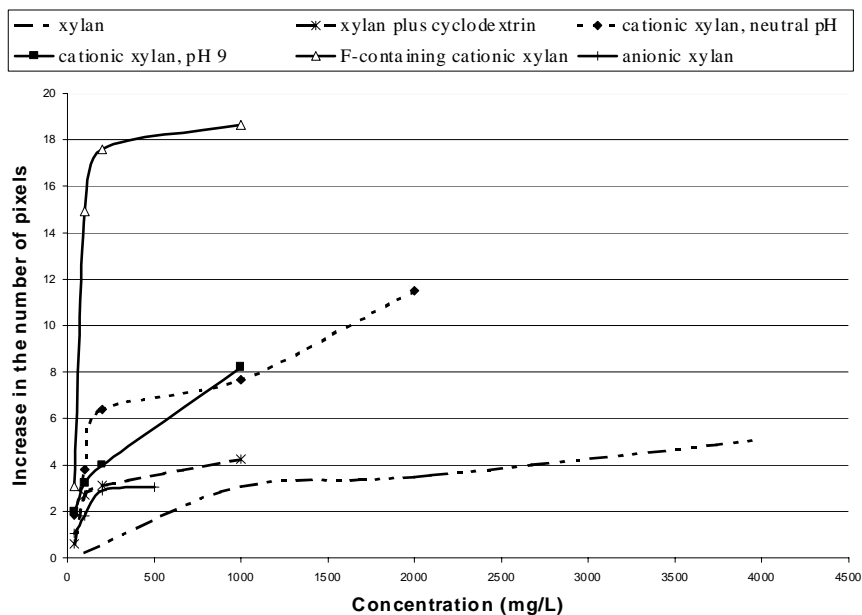


Figure 6. Results of an SPR-analysis monitoring film thickness (in pixels, whereby 2 pixels correspond approximately to 1 Å) on a concentration-scale for several xylan derivatives (peanut hull xylan served as starting material).

modified xylan is more strongly adsorbed by the cellulose surface with a sharp change in resonant angle to a value of approximately 8 pixels at concentrations below  $0.1 \text{ g L}^{-1}$  (Figure 6). Given the thickness of a cellulose layer,  $4.2 \text{ \AA}$  (34), this change in resonant angle, 8 pixels  $\approx 4 \text{ \AA}$ , maybe close to monolayer coverage. Another interesting feature is that anionic, cationic, and xylan plus cyclodextrin films all reach their plateau adsorption value below  $0.1 \text{ gL}^{-1}$  (Figure 6). Moreover, the driving force for enhanced adsorption of cationic xylan on cellulose does not seem to be solely driven by charge as the adsorbed amount was independent of pH over a limited but important range.

Enhanced adsorption (“docking”) was not unexpected as the cationic functional groups can ionically bond to surface anionic functionalities present on regenerated cellulose films. This phenomenon is an effect similar to cationically modified starch being used for paper sizing (35). Nonetheless, as noted above, this effect is smaller than expected, hence the CTP results drove us to also try incorporating F-substituents onto the cationic xylan.

Figure 6 also shows that the adsorption behavior of cationic xylan can be further enhanced by introducing F-containing functionality into the molecule. X-ray photoelectron spectroscopy (XPS) experiments used to obtain the amount of F present on the polymer provided an estimated degree of substitution (DS) of approximately 0.1 (i.e., 1 F-substituent per 10 anhydroxylose units). Hence, even a small amount of F-substituents causes a substantial change in the amount of cationic xylan adsorbed. Based on the change in resonant angle, 18 pixels, adsorbed layer, on the order of  $9 \text{ \AA}$ , forms at low bulk solution concentrations. Hence, both ionic and hydrophobic interactions must be important for xylan adsorption on cellulose surfaces.

**AFM Analysis of LB-Film Surfaces:** The use of the same films employed for SPR experiments in subsequent AFM-experiments was made impossible by the use of a refractive index-adjusting oil that was found to interfere with AFM observations. For this reason, separate LB-films of regenerated cellulose were used in adsorption experiments in which films on glass (instead of gold) slides were suspended in water-soluble polysaccharide solutions of different composition and different concentration. Each adsorption experiment lasted for several hours at room temperature, followed by thorough washing of the surface with deionized water. The resulting surfaces were examined by AFM in the height as well as the phase-mode. The results reveal different levels of adsorption for water-soluble polysaccharides in the form of film-like coatings or nanosize particles and agglomerates. The fluorinated cationic xylan derivative appears to produce a textured surface with nanosize particles (Figure 7). Hence, even though F-containing xylan showed the strongest adsorption (“docking”) behavior, the textured surface supports the conclusion that adsorption of the xylan derivatives produces submonolayer coverage, and that adsorption occurs largely through “micellar” aggregates.



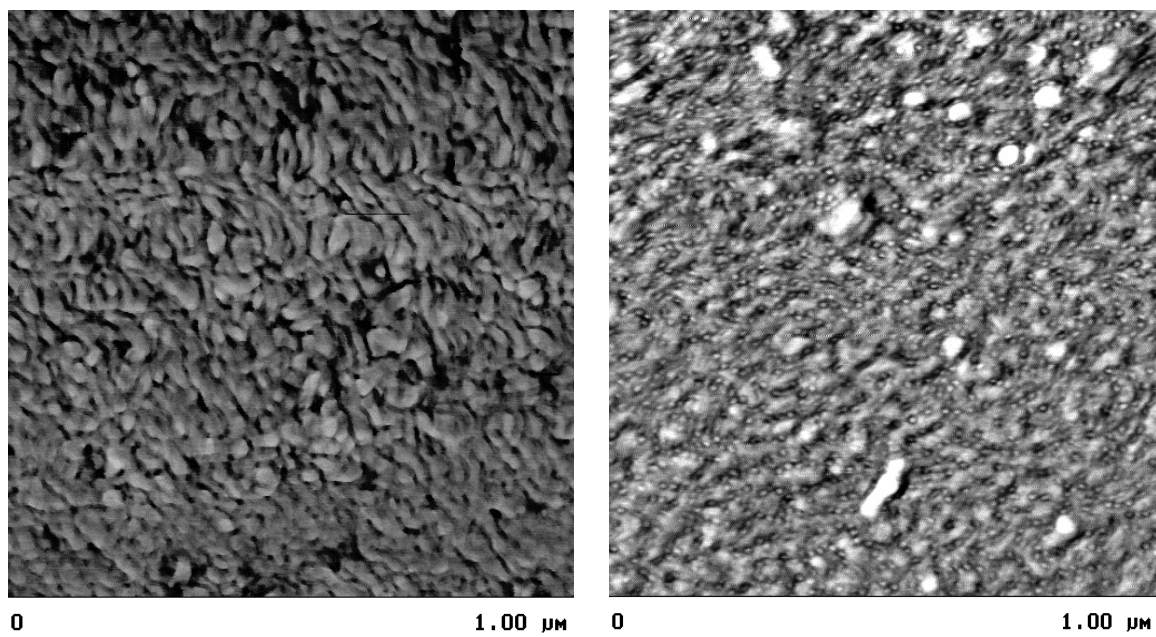


*Figure 7. AFM height image (left) and phase images (right) of a 40-layer cellulose LB film treated with an aqueous solution of the F-containing cationic xylan derivative. Note the spherical particles deposited on the image on the right side.*

### **Hypothetical Structures of Self-Assembled Micellar Aggregates:**

Various schematic models representing the possible structures of polysaccharidic and F-containing polymers have been advanced in the recent past. Some of these structures are illustrated in Figure 8. While it is too early to speculate on the specific structure of hemicellulose-like polysaccharides, it is apparent that both chemical structure and molecular size influence micellation, and this assembly is consistent with several of the aggregate models proposed for a variety of amphiphilic molecules.

The self-aggregation of telechelic copolymers with F-containing substituents has been pictured as the formation of jellyfish-like structures (7) in accordance with a proposition of Eisenberg et al. (4) (Figure 8A) for diblock copolymers. The extensive work on cholesteroylated pullulan (copolysaccharide) by Sunamoto et al. (12-15) has resulted in the model of a spherical nanoparticle transformed into a hydrogel by hydrophobic interactions (Figure 8B). Only one cholesteryl substituent in 100 anhydro-glucose repeat units of pullulan is sufficient to produce a gel structure. Uraki et al. (16, 17) present a similar vision for their hydroxypropylated unbleached organosolv pulp cellulose (Figure 8C). Recent work by Hillmyer and Lodge (11) advanced the idea of a self-aggregated structure varying with the magnitude of the polymer-polymer interaction parameter,  $\chi$ . Whether the phases of the copolymers separate weakly or strongly depends on values of both  $\chi$  and the molecular size of the respective copolymer components (in our case, the DP of the cellulose ester segment, Figure 5). A spherical aggregate structure results when the two copolymer components differ modestly in compatibility (i.e., have a low  $\chi$ -value), and a more oblate, disk-like or sheet-like structure will result when  $\chi$  rises (Fig. 8D). Thus, it can be expected that xylan-rich heteropolysaccharides produce self-aggregates with different structures, and that these differences depend on both molecular size and chemical structure, especially in relation to substitution patterns with non-polar groups.

## **Conclusions**

1. Mono-functional, F-terminated cellulose ester oligomers in THF were found to self-assemble into micellar structures at concentrations of between  $10^{-4}$  to  $10^{-5}$  moles  $L^{-1}$ . The CMC depended on both the chemical nature of the oligomer (i.e., type of F-containing end group) and the size of the CTP-segment.

2. Langmuir Blodgett (LB) films of regenerated cellulose represent a uniform and a highly ordered cellulose surface well-suited for adsorption studies.

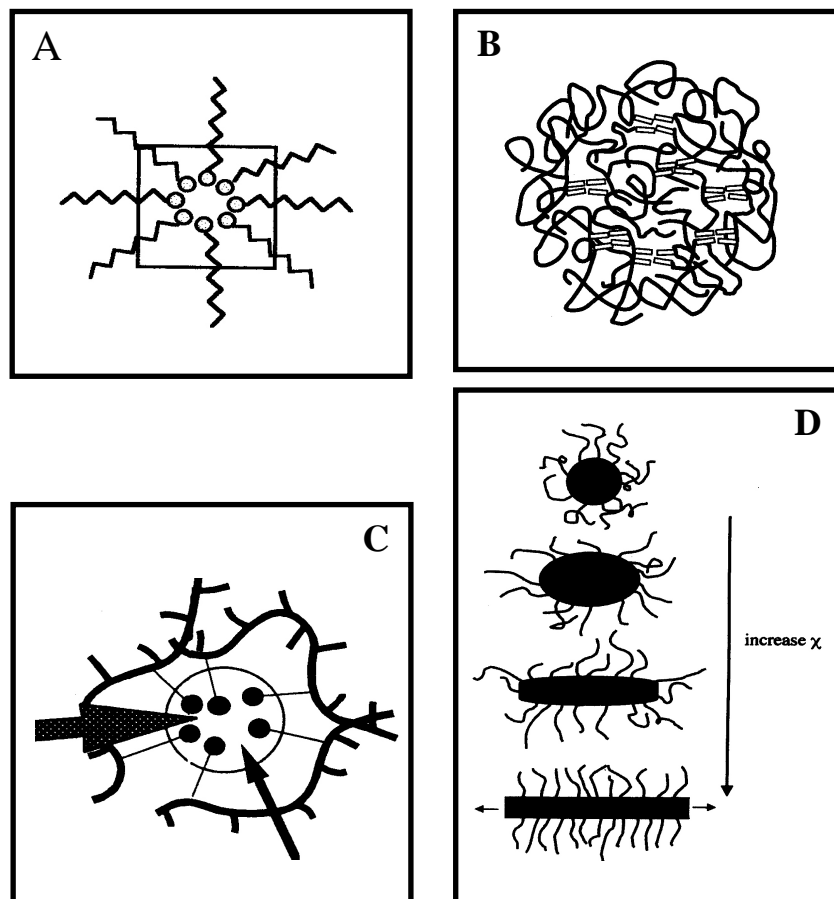


Figure 8. Several conceptual illustrations of the hypothetical structures of self-assembled macromolecular aggregates. (A) Micelles formed by blocky F-containing cellulose ester copolymers in THF-solution; (B) Schematic polycore model of cholesteroylated pullulan ; (C) self-aggregate of hydroxypropylated unbleached (acetic acid-based organosolv) pulp cellulose; and (D) micellar structures changing from spherical (top) to sheet-like (bottom) with increasing polymer-polymer interaction parameter ( $\chi$ ). ((A) Reproduced with permission from reference 7. Copyright 1998 American Chemical Society. (B) Reproduced with permission from reference 13. Copyright 1995 Japanese Academy. (C) Reproduced with permission from reference 16. Copyright 1997 Walter de Gruyter. (D) Reproduced with permission from reference 11. Copyright 2002 John Wiley & Sons, Inc.)

3. The adsorption of polysaccharide derivatives on LB-surfaces of cellulose can be studied by SPR in relation to solute structure and concentration.

4. The amount of adsorbed xylan (heteropolysaccharide) is promoted by cationic functionality as well as by enhancing the amphiphilic character with strongly hydrophobic (F-containing) substituents.

5. AFM images corroborate the SPR results and demonstrate the deposition of nano-particles on the cellulose surfaces with submonolayer coverage.

6. The results are consistent with a variety of hypothetical models of self-assembled structures that depend on both the chemical composition (i.e., compatibility of different copolymer components), as well as molecular size.

### Acknowledgment

Financial support for this study was provided by the USDA under its NRI program, contract # 9902352. Helpful discussion of the study by Prof. Paul Gatenholm and Hanno Roebroks, Chalmers University of Technology, are greatly appreciated.

### References Cited

1. Simmons, W. C. In *Smart Materials Technologies*. W. C. Simmons, I. A. Aksay, and D. R. Huston, eds. Proc. SPIE, SPIE:Bellingham, WA, Vol. 3040, **1997**, pg. 2-7.
2. Polla, D. L., W. P. Robbins, T. Tamagawa, C. Ye. *Mat. Res. Soc. Symp. Proc.*, 276, **1992**.
3. Bellare, J. R., T. Kaneko, and D. F. Evans. *Langmuir* 4, **1988**, 1066.
4. Zhang, L., H. Shen, and A. Eisenberg. *Macromolecules* 30, **1997**, 1001.
5. Lin, Z. *Langmuir* 12, **1996**, 1729.
6. Kikuchi, A., and T. Nose. *Polymer* 37(26), **1996**, 5889.
7. Becker, U., J. G. Todd, and W. G. Glasser. Surface Segregation Phenomena in Blends of Cellulose Esters. Chapter in Cellulose Derivatives: Modification, Characterization, and Nanostructures, Th. J. Heinze and W. G. Glasser, eds., ACS Symp. Ser. No. 688, 315-331 (**1998**).

8. Frazier, C. E., and W. G. Glasser. **1995**. Intramolecular effects in cellulose mixed benzyl ethers blended with poly( $\epsilon$ -caprolactone). *J. Appl. Polym. Sci.*, 58(6):1063-1075.
9. Sealey, J. E., C. E. Frazier, G. Samaranayake, and W. G. Glasser. **2000**. Novel cellulose derivatives. V. Synthesis and thermal properties of esters with trifluoroethoxy acetic acid. *J. Polymer Sci.: Pt. B: Polym. Physics* 38 (3), 486-494.
10. Glasser, W. G., U. Becker, and J. G. Todd. **2000**. Novel cellulose derivatives. VI. Preparation and thermal analysis of two novel cellulose esters with fluorine-containing substituents. *Carbohydrate Polymers* 42, 393-400.
11. Hillmyer, M. A., Lodge, T. P. Synthesis and self-assembly of fluorinated block copolymers. *J. Polymer Sci.: Pt. A*, 40, **2002**, 1-8
12. Sunamoto, J., Sato, T., Taguchi, T., and Hamazaki, H. Naturally occurring polysaccharide derivatives which behave as an artificial cell wall on an artificial cell liposome. *Macromolecules* 25, **1992**, 5665-5670.
13. Akiyoshi, K., S. Deguchi, H. Tajima, T. Nishikawa, and J. Sunamoto. Self-assembly of hydrophobized polysaccharide. *Proc. Japan Acad.* 71, **1995**, Ser. B, 15-19.
14. Akiyoshi, K., Taniguchi, I., Fukui, H., and Sunamoto, J. Hydrogel nanoparticle formed by self-assembly of hydrophobized polysaccharide. Stabilization of adriamycin by complexation. *Eur. J. Biopharm.* 42 (4), **1996**, 286-290.
15. Nishikawa, T., Akiyoshi, K., and Sunamoto, J. Macromolecular complexation between serum albumin and the self-assembled hydrogel nanoparticle of hydrophobized polysaccharides. *J. American Chem. Soc.* 118 (26), **1996**, 6110-6115.
16. Uraki, Y., K. Hashida, and Y. Sano. Self-assembly of pulp derivatives as amphiphilic compounds: Preparation of amphiphilic compound from acetic acid pulp and its properties as an inclusion compound. *Holzforschung* 51, **1997**, 91-97.
17. Uraki, Y., Hanzaki, A., Hashida, K., and Sano, Y. Self-assembly of pulp derivatives as amphiphilic compounds: verification of molecular association and complexation with low and high molecular mass compounds. *Holzforschung* 54, **2000**, 535-540.
18. Glasser, Wolfgang G., William E. Kaar, Rajesh K. Jain, and James E. Sealey. **2000**. Isolation options for non-crystalline heteropolysaccharides (HetPS).(Part 5 of "Steam-Assisted Fractionation of Biomass"-series). *Cellulose* 7(3), 299-317.
19. Henriksson, A., and P. Gatenholm. Controlled assembly of glucuronoxylans onto cellulose fibres. *Holzforschung* 55, **2001**, 494-502.

20. Petty, M. C. Langmuir-Blodgett films, an introduction. Cambridge University Press, **1996**.
21. Schaub, M., G. Wegner, G. Wenz, A. Stein and D. Klemm. Ultrathin films of cellulose on silicon wafers. *Advanced Materials* 5(12), **1993**, 919-923.
22. Basque, P., A. de Gunzbourg, P. Rondeau, and A. M. Ritcey. Monolayers of cellulose ethers at the air-water interface. *Langmuir* 12, **1996**, 5614-5619.
23. Loscher, F., T. Ruckstuhl, T. Jaworek, G. Wegner and S. Seeger. Immobilization of biomolecules on Langmuir-Blodgett films of regenerative cellulose derivatives. *Langmuir* 14(10), **1998**, 2786-2789.
24. Mao, L., and A. M. Ritcey. Preparation of cellulose derivative containing carbazole chromophore. *J. Appl. Polym. Sci.* 74, **1999**, 2764-2772.
25. Mao, L., and A. M. Ritcey. Langmuir-Blodgett films of cellulose ethers containing carbazole. *Macromol. Chem. Phys.* 201, **2000**, 1718-1725.
26. Green, R. J., R. A. Frazier, K. M. Shakesheff, M. C. Davies, C. J. Roberts, and S. J. B. Tandler. Surface plasmon resonance analysis of dynamic biological interactions with biomaterials. *Biomaterials* 21, **2000**, 1823-1835.
27. de Oliveira, W., and W.G. Glasser. **1994**. Novel cellulose derivatives. II. Synthesis and characteristics of mono-functional CP segments. *Cellulose*, 1(1), 77-86.
28. Glasser, W. G., and U. Becker. **1999** (app'd in 2000). About the hydrolysis of cellulose propionate to segments with low DP. *Cellulose* 6(4), 283-28.
29. Pulkkinen, E., A. Maekelae, and H. Makkonen. Preparation and testing of cationic flocculants from Kraft lignin. In *Lignin – Properties and Materials*, W. G. Glasser and S. Sarkanen, eds., ACS Symp. Ser. No. 397, **1989**, 284-293.
30. Gustavsson, M., M. Bengtsson, P. Gatenholm, W. Glasser, A. Teleman, and O. Dahlman. Isolation, characterisation and material properties of 4-O-methylglucuronoxylan from aspen. Chapter in *Biorelated Polymers – Sustainable Polymer Science and Technology*, E. Chiellini, H. Gil, G. Braunegg, J. Buchert, P. Gatenholm, and M. van der Zee, Eds., Kluwer Academic/Plenum Publishers, New York, **2001**, pg. 41-52.
31. Evans, D., and H. Wennerstrom. *The colloidal domain*. Wiley-VCH, **1999**.

32. Davey, T. W., W. A. Ducker, and A. R. Hayman. 2000. Aggregation of  $\omega$ -Hydroxy Quaternary Ammonium Bolaform Surfactants. *Langmuir* 16, 2430-2435.
33. Jain, Rajesh K., M. Sjöstedt, and W. G. Glasser. **2001**. Thermoplastic xylan derivatives with propylene oxide. *Cellulose* 7(4), 319-336.
34. Buchholz, V., G. Wegner, S. Stemme, and L. Oedberg. *Adv. Mater.* 8, **1996**, 399-402.
35. Maximova, N., Laine, J., and Stenius, P. Adsorption of lignin-cationic starch complexes on the cellulose fibers. *Proc. 7<sup>th</sup> European Workshop on Lignocellulosics and Pulp, Turku/Abo, Finland, August 26-29, 2002*, 127-130.

## **Appendix 2**



# **SURFACE MODIFICATION OF CELLULOSE FIBERS -TOWARDS WOOD COMPOSITES BY BIOMIMETICS**

Sheila E. Gradwell<sup>1</sup>, Scott Rennecker<sup>2</sup>, Alan R. Esker<sup>1</sup>, Thomas Heinze<sup>3</sup>,  
Paul Gatenholm<sup>4</sup>, Carlos Vaca-Garcia<sup>5</sup>, and Wolfgang Glasser<sup>2</sup>

<sup>1</sup>Department of Chemistry, Virginia Tech, Blacksburg, Virginia, 24061 USA

<sup>2</sup>Department of Wood Science and Forest Products, Virginia Tech, Blacksburg, Virginia,  
24061 USA

<sup>3</sup>Institut für Organische Chemie and Makromolekulare Chemie, Friedrich-Schiller-  
Universität of Jena, Humboldtstrasse 10, D-07743 Jena, Germany

<sup>4</sup>Department of Materials and Surface Chemistry, Chalmers University of Technology,  
SE-412 96 Göteborg, Sweden

<sup>5</sup>ENSIACET, Institut National Polytechnique de Toulouse, Toulouse, France

## Abstract

A biomimetic approach was taken for studying the adsorption of a model copolymer (pullulan abietate, DS 0.027) representing the lignin-carbohydrate complex to a model surface for cellulose fibers (Langmuir-Blodgett thin films of regenerated cellulose). Adsorption results were assayed using surface plasmon resonance spectroscopy (SPR) and atomic force microscopy (AFM). Rapid, spontaneous, and desorption-resistant surface modification resulted. This effort is viewed as a critical first step towards the permanent surface modification of cellulose fibers with a layer of molecules amenable to either enzymatic crosslinking for improved wood composites or thermoplastic consolidation.

Notice- This is a preprint of an article accepted for publication in *Comptes Rendus Biologie* © 2004.

## 1. Introduction

Wood composites are a class of materials that generally consist of solid fragments of wood that are reconstituted in a form fit for a designated end-use by some sort of adhesion process. Plywood, fiber boards, particleboard, oriented strand board (OSB), and wood plastic composites are all members of this class of composites [1]. Over time, wood composites have been reconstituted from ever-smaller wood fragments, progressing from plies to strands to fibers to fine “flour” measuring only microns in size. The latter represent the dimensions of wood fragments typically used for wood plastic composites produced by thermal extrusion processes [2]. Wood composites are capturing ever-larger markets, partially in response to reductions in the supply of solid, large dimension timber [3, 4].

Composites in general are materials that combine the high strength and stiffness characteristics of a fiber (or particle) with the ductility of a (continuous) matrix [5]. In many man-made composites the fiber-matrix interface is the weakest point resulting in “fiber pull-out” and failure before the fiber reaches its true strength potential [6]. In wood plastic composites, the dimensions of the wood fibers (if they existed in fiber form in the first place) often suffer a significant loss of aspect ratio caused by the high shear forces of the extruder at high temperatures [7]. Many wood composites also suffer from the high density that is the result of thermal processing under high-pressure conditions [8, 9]. The ideal wood-like composite would combine the features of a high-strength and high-stiffness (hollow) fiber embedded in a continuous matrix from which it never (under any condition of moisture or temperature) separates interfacially, and with which it produces a lightweight material [10, 11]. That is to say, *wood* in its native state is an ideal composite; a material worth mimicking! This conclusion has been recognized by a recent report of the National Academy of Sciences of the USA, which advocates the use of the “*hierarchical structures in biology as a guide for new materials technology*” [12].

In order to adopt the principles of biomimetics to the process of composite formation from wood fibers, two crucial elements must be understood. First, how can a matrix (i.e., lignin)-rich layer be deposited on the surface of a cellulose fiber? Second, how can this

layer of matrix material be consolidated to form an adhesive bond between fibers? Solutions to these problems may potentially be accomplished thermally or biologically, i.e., by biomimetics.

Thermoplastic cellulose composites may potentially be formed when cellulose fibers are surface-coated with melt-deformable copolymers. Such copolymers may consist of saccharidic amphiphiles containing waxy substituents. Cellulose and/or cellulose derivatives have served as both adsorbing surface substrates and adsorbable amphiphiles [13-24]. Employing this established method of surface modification using amphiphilic copolymers with olefinic character, a thermoplastic coating may be produced on cellulose fiber surfaces. Cellulose mono- and di-esters with long chain fatty acids have recently been shown to represent thermoplastic entities with melting/softening points that decline in accordance with methylene group content (Fig. 1) [25,26]. Thus, melt-processable cellulose esters with low degrees of substitution (DS) may potentially open a route towards thermoplastic fiber composites by adsorption processes.

A biology-mimicking approach may involve the surface adsorption of molecules amenable to enzymatic crosslinking. During secondary wall formation in wood cells, cellulose is spun from rosette structures into an aqueous sol-like hemicellulose solution [27]. There is a body of work describing how hemicelluloses regulate (bacterial) cellulose fibril diameter [28-33]. These studies demonstrate that adsorption of heteropolysaccharides plays a key role in establishing an interfacial region that prevents delamination and fiber pull-out in wood. This adsorption process is governed by self-assembly, a process driven by thermodynamics that results in the aggregation of bipolar molecules on the fiber surface. Self-assembly behavior has been observed with many other natural amphiphilic polymers including oligosaccharide-protein block copolymers [34], hydroxyethyl cellulose [35,36], fluorine-containing cellulose diblock structures, xylan-rich heteropolysaccharides and their derivatives [37], and lignin-carbohydrate complexes [38,39].

Our studies were motivated by a vision of biomimetics. They presume that a cellulose surface enriched with lignin or lignin precursors becomes susceptible to the generation of phenoxy radicals by enzyme catalysis. Free radicals then form network polymers (thermoset adhesives) by coupling [40]. Felby et al. [41-45] and Huettermann et al. [46-53] have shown that wood fibers can be enzymatically activated *in vitro* with phenoloxidase and/or laccase, and this treatment can be used to produce wood composites with enhanced auto-adhesion between components [47,51]. The lignin-coated fibers that are formed when a lignin-carbohydrate complex is adsorbed to a cellulose surface may possess the potential for enzymatic activation and the development of adhesive bonds that are similar to those in wood.

This report describes some basic experiments to demonstrate how a model cellulose surface (which is devoid of the complexities that porosity, microfibril orientation, fiber dimension, etc. entail) and a model lignin-carbohydrate copolymer complex (which is devoid of the complexities of molecular non-uniformity, size, and structure) interact under conditions that often produce self-assembly.

## 2. Materials and Methods

### 2.1. Cellulose Model Film Preparation

Smooth, uniform films of regenerated cellulose were prepared on 12 mm x 12 mm SPR sensor slides using a protocol adapted from Schaub et al. [54] and previously described in conjunction with a study on the adsorption of lignin-containing hemicellulose derivatives [37]. Each sensor slide (Reichert, Inc.) consisted of a glass slide covered with 1 nm of chromium and 50 nm of gold. Each slide was cleaned by immersion in a 7:3 solution of concentrated sulfuric acid:hydrogen peroxide (30%) for 30 minutes. The glass portion of the sensor slide was hydrophobized by exposure to 1,1,1,3,3,3-hexamethyldisilazane in an 80°C oven for 6 hours. Upon cooling, the slide was placed into a 1mM solution of 1-dodcanethiol (Aldrich) in absolute ethanol for 2 hours according to a procedure described by Laibinis et al. [55]. Trimethylsilyl (TMS) cellulose (Jena Biosciences, Ltd.) was spread from a solution of 5 mg of polymer in 10 ml of chloroform onto the water surface of a Langmuir-Blodgett (LB) trough (KSV 2000) and transferred accordingly to prepare

films 20 layers in thickness. TMS cellulose was removed from the glass side of the sensor slide using chloroform. Cellulose was regenerated by exposure of the film to gaseous wet HCl for 30 seconds [54].

## 2.2. Lignin-Carbohydrate Copolymer Synthesis

The lignin-carbohydrate complex was modeled using a high molecular weight pullulan (water-soluble polysaccharide) derivatized with abietic acid (Fig. 2). The derivatization involved reacting pullulan with the acyl chloride of abietic acid in the presence of pyridine. The degree of substitution (DS) was approximately 0.027, or one abietic (non-polar) substituent per every 37 anhydroglucose units. The protocol was adopted from the work of Sunamoto et al. [18].

## 2.3. Surface Tension Measurements

Surface tension measurements of aqueous pullulan and pullulan abietate solutions were conducted using the tensiometer from a Langmuir-Blodgett trough (KSV 2000). The surface tension was determined by the Wilhelmy plate technique using a sand-blasted platinum plate. Each solution was placed in a specially designed glass jar that consisted of an inner cup containing the solution and an outer jacket which allowed for insulation with 22.5°C water flowing from a circulating thermostated bath.

## 2.4. Surface Adsorption and Desorption Tests

The docking behavior of pullulan abietate, DS=0.027, onto a regenerated cellulose surface was investigated using surface plasmon resonance (SPR) spectroscopy. The SPR sensor slide was refractive index-matched to the prism of the Leica AR 700 automatic refractometer using immersion oil ( $n_D = 1.5150$ ). The flow cell body was equipped with a Viton gasket (Dupont Dow Elastomers LLC) and mounted on top of the sensor slide. Solutions were pumped into the flow cell at a flow rate of 0.35 mL•min<sup>-1</sup> via PEEK tubing (Upchurch Scientific) connected to a cartridge pump (Masterflex). Prior to data acquisition, the cellulose surface was allowed to reach equilibrium swelling by flowing only Milli-Q water through the system. Once a stable baseline was established, solution containing the amphiphile was pumped into the flow cell. Each solution was allowed to

flow for 20 minutes before switching to water via a solvent selection valve. Water was allowed to flow until a new baseline was established, as the signal did not return to the original baseline due to irreversible adsorption of the pullulan abietate. Solutions of higher concentration were run through the flow cell under the same conditions described above. It should be noted that once surface saturation occurs, molecules can adsorb onto material already docked to the surface.

### 2.5. Surface Analysis

Atomic Force Microscopy (AFM) images were obtained for regenerated cellulose, pullulan on cellulose, and pullulan abietate on cellulose. Pullulan and pullulan abietate were adsorbed onto their respective substrates by submersion into solutions at the critical aggregation concentration of each material. Substrates were rinsed with Milli-Q water and dried with nitrogen prior to analysis. Measurements were conducted in tapping mode on a Digital Instruments Dimension 3000 Scope with a Nanoscope IIIa controller using silicon cantilevers and tips.

### 2.6. Other Characterizations

Ultraviolet-visible spectroscopy was used to quantify the degree of substitution of pendant abietate groups on pullulan abietate. Solutions were prepared in a mixed solvent system composed of 44% water and 56% methanol by volume and analyzed using a Varian Cary 50 Bio UV-Visible Spectrophotometer.

## 3. Results and Discussion

The lignin-carbohydrate complex consists of a family of copolymers that varies widely in composition. Discernible gradients exist with regard to the chemical (unit type and concentration) as well as physical (size, molecular weight, degree of crosslinking) structure of this complex across the space between fibers (middle lamella). There is no single copolymer structure that can represent this complex. In order to examine the behavior of hemicellulose-like molecules carrying lignin-like hydrophobic moieties in terms of their self-assembly behavior at cellulose surfaces, a well-characterized pullulan abietate (PA) (DS=0.027) was synthesized that represents a variant of the

cholesteroylated pullulan used by Sunamoto et al. [13-20]. The PA prepared produced an NMR spectrum which was non-descriptive in terms of DS on account of the low abietate content. However, UV-spectroscopy provided clear evidence about the degree of substitution of the diterpene (Fig. 3).

The self-assembly behavior of the amphiphilic PA in water was examined by surface tension measurements. It is unlikely that PA forms traditional “micelles” due to the low degree of substitution. This reason is why the term “aggregate” will be used to describe these self-assembled structures. In Figure 4, the critical aggregation concentration (cac)-value of PA is compared to un-derivatized pullulan (P). Although the transition from non-aggregated to aggregated solution occurs over a range of concentrations, it is evident that (a) the presence of PA has a more dramatic effect on the surface tension of water, and (b) PA’s cac occurs at a significantly lower concentration than that of the corresponding P-control. These observations indicate that the copolymer aggregates more readily than its parent polysaccharide due to the presence of the diterpene substituents.

The aggregation behavior of the PA in the presence of a solid cellulose surface was examined by surface plasmon resonance (SPR) spectroscopy. SPR is capable of detecting the docking event by a single molecule at thin film surfaces [56-60], and it has previously been employed for measuring the relative rate of adsorption of water-soluble oligo- and polysaccharides at cellulose surfaces [37]. The data recorded illustrate that PA adsorbs to cellulose LB film surfaces rapidly, in significant quantities, and remains mostly desorption-resistant (Fig. 5). To test the final feature, flow-through experiments with PA solutions at concentrations below the cac are alternated with those of pure (deionized) water for time periods of >20 min, the adsorption/desorption process reveals the build-up of a layer of copolymer at the surface that can not be removed (within the time period examined) by washing with water.

The results of this adsorption can be visualized by atomic force microscopy (AFM) (Fig. 6). Comparing the control LB-surface with one that had been in contact with P and one that was present during PA flow (at a concentration equal to the cac), the surface

roughness-values revealed significant differences. Whereas surface roughness increased by 40% following contact with P, the roughness rose by 160% when the amphiphilic copolymer was present in solution. Noteworthy is that, with minimal substitution (DS=0.027) of the PA, the decrease in water's solvent quality caused by a few abietic acid groups is enough to promote the adsorption of the copolymer to a higher degree than the unsubstituted pullulan. This effect suggests that the degree of roughness can be controlled by the degree of substitution of the copolymer with hydrophobic moieties; and hence, the interphase thickness of a composite can be controlled over a significant range. Overall, these results indicate a propensity of cellulose surfaces to adhere spontaneously to carbohydrate-based amphiphiles in an aqueous environment similar to what is found during secondary cell wall synthesis in woody plants. This process is depicted in Figure 7 with respect to the cac. During initial exposure of the amphiphile to the cellulose surface (a), chains adsorb with a loop-tail conformation. The presence of abietic acid groups drives the deposition of material from the bulk onto exposed abietic acid groups on the surface (b-c). Once a solution, whose concentration is above the cac, is introduced into the system, aggregates begin to form in the bulk (d). These aggregates are also capable of docking to material on the surface (e-f). Due to the inability to desorb pullulan abietate by rinsing with water, this material seems to be adaptable for convenient and practical surface modification of cellulose films and fibers.

These results support the hypothesis that cellulose surfaces can be modified by the adsorption of self-assembled amphiphilic copolymers based on polysaccharides. If the hydrophobic character of the copolymers were to represent (a) a waxy (thermoplastic) substance, or (b) a phenolic (crosslinkable) entity (rather than a diterpenoid moiety), a fiber would result that would be amenable to thermal or enzymatic consolidation and composite preparation, respectively.

#### 4. Conclusions

Cellulose (fiber) surface modification with cross-linkable, lignin-like copolymers, or thermoplastically-deformable copolymers, on the basis of water-soluble carbohydrates is envisioned as a critical step for the preparation of wood composites by biomimetics. A series of adsorption experiments were carried out that involved the self-deposition of



water-soluble pullulan abietate derivatives (as models for a lignin-carbohydrate copolymer complex) on Langmuir-Blodgett films of regenerated cellulose (as models for cellulose fiber surfaces). The results indicated a significant, spontaneous, and apparently desorption-resistant modification of the cellulose surface by copolymer. This type of surface modification is seen as a critical biomimetic step for the creation of stronger composite interfaces involving cellulose fibers.

## 5. Acknowledgment

Financial support for this study was provided by the United States Department of Agriculture as part of its NRI program, contract # 9902352; and by the National Science Foundation, # CHE-0239633, which allowed for the purchase of the SPR. The authors wish to thank Mr. Muhammed Ajaz Hussain, University of Wuppertal, Germany for the preparation of the lignin-carbohydrate copolymer, Dr. Ray Dessy and Miss Aysen Tulpar, Virginia Tech for guidance in the field of surface plasmon resonance, and Dr. Stephen McCartney, Virginia Tech for assistance with atomic force microscopy.

## References

1. Youngquist, J., Wood-based composite panel products, In Wood Handbook: Wood as an Engineering Material, Forest Products Society USA, (1999) 10-1.
2. Clemons, C., Wood-plastic composites in the United States - The interfacing of two industries, Forest Prod. J. 52 (2002) 10-18.
3. Anon., \$900 million market for natural and wood fiber plastic composites in North American and Europe according to new Principia Partners study, Business Wire, (2002).
4. Shook, S. and I. Eastin, A Characterization of the U.S. Residential Deck Material Market, Forest Prod. J. 51 (2001) 28-36.
5. Gordon, J.E. and G. Jeronimidis, Composites with high work of fracture, Phil. Trans. R. Soc. Lond. A 294 (1980) 545-550.

6. Harris, B., The mechanical behavior of composite materials, In The mechanical properties of biological materials, Symposia for the Society for Experimental Biology, J.F.V. Vincent and J.D. Currey, Editors, Cambridge University Press (1980) 37-74.
7. Sperber, V. E., University of Kassel, Germany, Personal communication.
8. Sanadi, A.R., D.F. Caulfield, and R.E. Jacobson, Agro-fiber thermoplastic composites, In Paper and Composites from Agro-based Resources, R. Rowell, R. Young, and J. Rowell, Editors, CRC Press, Inc.: USA (1997) 391.
9. Sheldon, R.P., Composite Polymeric Materials: Applied Science Publishers LTD. (1982) 141.
10. Bond, G.M., R.H. Richman, and W.P. McNaughton, Mimicry of Natural Material Designs and Processes, Journal of Materials Engineering and Performance 4 (1995) 334-342.
11. Srinivasan, A.V., G.K. Haritos, and F.L. Hedberg, Biomimetics: Advancing man-made materials through guidance from nature, Appl. Mech. Rev. 44 (1991) 463-482.
12. National Academy of Science, Hierarchical structures in biology as a guide for new materials technology, Washington, D.C.: National Academy Press. (1994) 130.
13. Akiyoshi, K., S. Yamaguchi, J. Sunamoto. Self-aggregates of hydrophobic polysaccharide derivatives. Chemistry Letters 7 (1991) 1263-1266.
14. Akiyoshi, K., K. Nagai, T. Nishikawa, J. Sunamoto. Self-aggregates of hydrophobized polysaccharide as a host for macromolecular guests. Chemistry Letters 9 (1992) 1727-1730.
15. Akiyoshi, K., J. Sunamoto. Physicochemical characterization of cholesterol-bearing polysaccharides in solution. Surfactant Sci. Ser. 44 (1992) 289-304.
16. Akiyoshi, K., S. Deguchi, N. Yamaguchi, J. Sunamoto. Self-aggregates of hydrophobized polysaccharides in water. Formation and characteristics of nanoparticles. Macromolecules 26(12) (1993) 3062-3068.

17. Guo, Z.-J., S. Kallus, K. Akiyoshi, J. Sunamoto. Artificial cell wall for plant protoplasts. Coating of plasma with hydrophobized polysaccharides. *Chemistry Letters* 6 (1995) 415-416.
18. Akiyoshi, K., S. Deguchi, H. Tajima, T. Nishikawa, and J. Sunamoto, Self-assembly of hydrophobized polysaccharides, *Proc. Japan Acad. Ser. B* 71 (1995) 15-19.
19. Kang, E.-C., Akiyoshi, J. Sunamoto. Surface coating of liposomes with hydrophobized polysaccharides. *J. Bioactive and Compatible Polymers* 12(1) (1997) 14-26.
20. Kuroda, K., K. Fujimoto, J. Sunamoto, A. Kazunari. Hierarchical self-assembly of hydrophobically modified pullulan in water: Gelation by networks of nanoparticles. *Langmuir* 18(10) (2002) 378-3786.
21. Kawaguchi, T., H. Nakahara, K. Fukuda. Mono- and multilayers of amphiphilic cellulose esters and some novel comblike polymers. *J. Colloid Interface Sci.* 104(1) (1985) 290-293.
22. Sundari, C. S., B. Raman, D. Balasubramanian. Hydrophobic surfaces in oligosaccharides: linear dextrans are amphiphilic chains. *Biochimica et Biophysica Acta* 1065(1) (1991) 35-41.
23. Shubin, V. Adsorption of cationic polymer onto negatively charged surfaces in the presence of anionic surfactant. *Langmuir* 10(4) (1994) 1093-1100.
24. Frechet, J. M. J., I. Gitsov, T. Monteil, S. Rochat, J.-F. Sassi, C. Vergelati, D. Yu. Modification of surfaces and interfaces by non-covalent assembly of hybrid linear-dendritic block copolymers: poly(benzyl ether) dendrons as anchors for poly(ethylene glycol) chains on cellulose or polyester. *Chem. Materials* 11(5) (1999) 1267-1274.
25. Vaca-Garcia, C., G. Gozzelino, W. G. Glasser, M. E. Borredon. Dynamic mechanical thermal analysis transition of partially and fully substituted cellulose fatty esters. *J. Polym. Sci.: Polym. Phys.* 41 (2003) 281-288.
26. Vaca-Garcia, C., J. Bras, E. Borredon, W. Glasser. The internal plasticization of long-chain cellulose esters (LCCE) by methylenic groups. Manuscript submitted.

27. Inomata, F., K. Takabe, and H. Saiki, Cell wall formation of conifer tracheid as revealed by rapid-freeze and substitution methods, *J. Electron Microsc.* 41 (1992) 369-374.
28. Atalla, R., J. Hackney, I. Uhlin, and N. Thompson, Hemicelluloses as structure regulators in the aggregation of native celluloses, *International Journal of Biological Macromolecules* 15 (1993) 109-112.
29. Iwata, T., L. Indrarti, and J. Azuma, Affinity of hemicellulose for cellulose produced by *Acetobacter xylinum*, *Cellulose* 5 (1998) 215-228.
30. Tokoh, C., K. Takabe, M. Fujito, and H. Saiki, Cellulose synthesized by *Acetobacter xylinum* in the presence of acetyl glucomanan, *Cellulose* 5 (1998) 249-261.
31. Uhlin, K., R. Atalla, and N. Thompson, Influence of hemicelluloses on the aggregation patterns of bacterial celluloses, *Cellulose* 2 (1995) 129-144.
32. Whitney, S., J. Brigham, A. Darke, J. Reid, and M. Gidley, *In vitro* assembly of cellulose/xyloglucan networks: ultrastructural and molecular aspects, *The Plant Journal* 8 (1995) 491-504.
33. Whitney, S., J. Brigham, A. Darke, J. Reid, and M. Gidley, Structural aspects of the interaction of mannan-based polysaccharides with bacterial cellulose, *Carbohydrate Research* 307 (1998) 299-309.
34. Hirai, M., T. Takizawa, S. Yabuki, T. Hirai, and K. Hayashi, Thermotropic Structural Change of Disialoganglioside Micelles Studied by Using Synchrotron Radiation Small-Angle X-ray Scattering, *J. Phys. Chem.* 100 (1996) 11675-11680.
35. Winnick, F., S. Regismond, and E. Goddard, Interactions of an Anionic Surfactant with a Fluorescent-dye-labeled Hydrophobically-modified Cationic Cellulose Ether, *Langmuir* 13 (1997) 111-114.
36. Sau, A.C. and L.M. Landoll, Synthesis and Solution Properties of Hydrophobically Modified (Hydroxyethyl)cellulose, In *Polymers in Aqueous Media: Performance Through Association*, *Advances in Chemistry Series No. 223*, J.E. Glass, Editor (1989) 343-363.

37. Esker, A.R., W.G. Glasser, U. Becker, S. Jamin, S. Beppu, and S. Rennecker, Self-Assembly Behavior of Some Co- and Heteropolysaccharides Related to Hemicelluloses, In Hemicelluloses: Science and Technology, ACS Symposium Series No. 864, P. Gatenholm and M. Tenkanen, Editors, American Chemical Society: Washington, DC (2003) 198-219.
38. Yaku, F., S. Tsuji, and T. Koshijima, Lignin Carbohydrate Complex. Pt. III. Formation of Micelles in the Aqueous Solution of Acidic Lignin Carbohydrate Complex, *Holzforschung* 33 (1979) 54-59.
39. Johnson, K.G. and R.P. Overend, Lignin-Carbohydrate Complexes from *Populus deltoides* I. Purification and Characterization, *Holzforschung* 45 (1991) 469-475.
40. Glasser, W.G., and S.S. Kelley. Lignin Section, *Encyclopedia of Polymer Science and Engineering*, Vol. 8, John Wiley & Sons, Inc., 795-852 (1987).
41. Felby, C., L.S. Pedersen, and B.R. Nielsen, Enhanced Auto Adhesion of Wood Fibers Using Phenol Oxidases, *Holzforschung* 51 (1997) 281-286.
42. Felby, C., B. R. Nielsen, P. O. Olesen, L. H. Skibsted. Identification and quantification of radical reaction intermediates by electron spin resonance spectrometry of laccase-catalyzed oxidation of wood fibers from beech (*Fagus sylvatica*). *Appl. Microbiol. Biotech.* 48(4) (1997) 459-464.
43. Felby, C., P.O. Olesen, and T.T. Hansen, Laccase Catalyzed Bonding of Wood Fibers, In *Enzyme Applications in Fiber Processing*, ACS Symposium Series 687, K.-E.L. Eriksson and A. Cavaco-Paulo, Editors, American Chemical Society: Washington, DC (1998) 88-98.
44. Felby, C., J. Hassingboe, and M. Lund, Pilot-scale production of fiberboards made by laccase oxidized wood fibers: board properties and evidence for cross-linking of lignin, *Enzyme and Microbial Technology* 31 (2002) 736-741.
45. Lund, M., M. Eriksson, and C. Felby, Reactivity of a Fungal Laccase Towards Lignin in Softwood Kraft Pulp, *Holzforschung* 57 (2003) 21-26.
46. Kharazipour, A., A. Huettermann, and H.D. Luedemann, Enzymatic activation of wood fibres as a means for the production of wood composites, *J. Adhesion Sci. Technol.* 11 (1997) 419-427.

47. Haars, A., A. Kharazipour, H. Zanker, and A. Huettermann, Room-Temperature Curing Adhesives Based on Lignin and Phenoloxidases, In Adhesives from Renewable Resources, ACS Symposium Series No. 385, R.W. Hemingway and A.H. Conner, Editors, American Chemical Society: Washington, DC (1989) 126-134.
48. Kharazipour, A., A. Haars, M. Shekholeslami, A. Huettermann. Enzyme-bonded wood materials based on lignin and phenol oxidases. *Adhaesion* 35(5) (1991) 30, 33-34, 36.
49. Milstein, O., A. Huettermann, A. Majcherczyk, K. Schulze, R. Freund, H. D. Luedemann. Transformation of lignin-related compounds with laccase in organic solvents. *J. Biotechnol.* 30(1) (1993) 37-47.
50. Milstein, O., A. Huettermann, R. Frund, H.-D. Luedemann. Enzymic co-polymerization of lignin with low-molecular mass compounds. *Appl. Microbiol. Biotech.* 40(5) (1994) 760-767.
51. Kharazipour, A., K. Schindel, and A. Hüttermann, Enzymatic Activation of Wood Fibers for Wood Composite Production, In Enzyme Applications in Fiber Processing, ACS Symposium Series 687, K.-E.L. Eriksson and A. Cavaco-Paulo, Editors, American Chemical Society: Washington, DC (1998) 99-115.
52. Kharazipour, A., K. Bergmann, K. Nonninger, A. Huettermann. *J. Adhesion Sci. Technol.* 12(10) (1998) 1045-1053.
53. Mai, C., A. Huettermann. Fungal laccase grafts acrylamide onto lignin in presence of peroxides. *Appl. Microbiol. Biotechnol.* 51(4) (1999), 527-531.
54. Schaub, M., G. Wenz, G. Wegner, A. Stein, and D. Klemm, Ultrathin Films of Cellulose on Silicon Wafers, *Advanced Materials* 5 (1993) 919-922.
55. Laibinis, P.E., G.M. Whitesides, D.L. Allara, Y.-T. Tao, A.N. Parikh, and R.G. Nuzzo, Comparison of the Structures and Wetting Properties of Self-Assembled Monolayers of n-Alkanethiols on the Coinage Metal Surfaces, Cu, Ag, Au, *J. Am. Chem. Soc.* 113 (1991) 7152-7167.
56. Brockman, J.M., B.P. Nelson, and R.M. Corn, Surface Plasmon Resonance Imaging Measurements of Ultrathin Organic Films, *Annu. Rev. Phys. Chem.* 51 (2000) 41-63.

57. Green, R.J., R.A. Frazier, K.M. Shakesheff, M.C. Davies, C.J. Roberts, and S.J.B. Tandler, Surface Plasmon Resonance Analysis of Dynamic Biological Interactions with Biomaterials, *Biomaterials* 21 (2000) 1823-1835.
58. Liedberg, B., C. Nylander, and I. Lundström, Biosensing with surface plasmon resonance - how it all started, *Biosensors & Bioelectronics* 10 (1995) i-ix.
59. Lundström, I., Real-time biospecific interaction analysis, *Biosensors & Bioelectronics* 9 (1994) 725-736.
60. Schuck, P., Use of Surface Plasmon Resonance to Probe the Equilibrium and Dynamic Aspects of Interactions Between Biological Macromolecules, *Annu. Rev. Biophys. Biomol. Struct.* 26 (1997) 541-566.

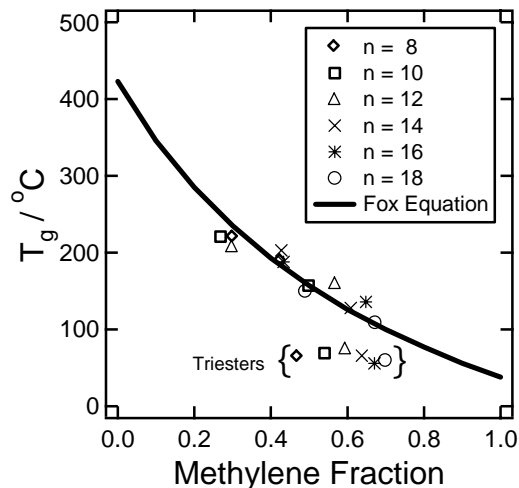


Figure 1. Glass transition temperatures ( $T_g$ ) of long-chain cellulose mono-, di-, and tri-esters (LCCE) with fatty acid substituents as a function of the methylene content (in weight-%) of the ester substituent. The methylene content of acetate groups is thereby considered nil, and that of a propionate group is 1. The number of carbon atoms in the substituent, the acyl group size, is given by  $n$ . Only mono- and di-esters follow the Fox equation, triesters have a constant glass transition at around 70-80°C. (According to data by Vaca-Garcia et al. [51]).



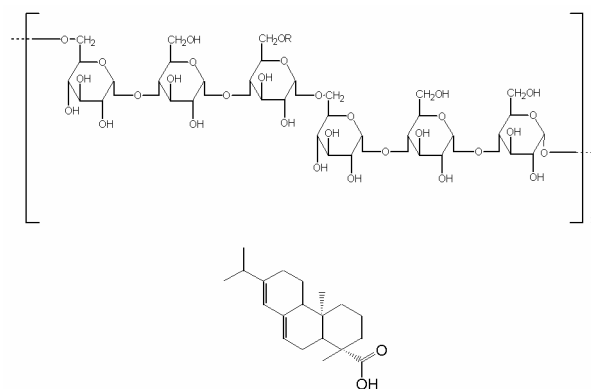


Figure 2. Structures of pullulan and abietic acid. The average degree of substitution used in this study is one abietic acid ester per 37 anhydroglucose linkages.

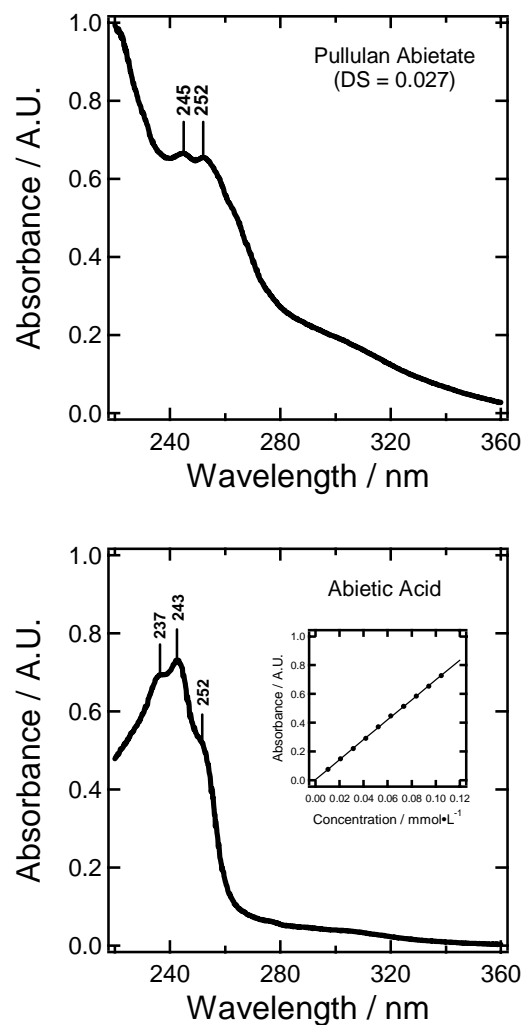


Figure 3. UV spectra of pullulan abietate ( $574 \text{ mg}\cdot\text{L}^{-1}$ ,  $\text{DS}=0.027$ ) and abietic acid ( $22.1 \text{ mg}\cdot\text{L}^{-1}$ ) in a mixed solvent system composed of 44% water and 56% methanol by volume. Un-derivatized pullulan does not absorb in this region. The calibration curve of abietic acid (inset) provided an estimate for the molar absorptivity ( $\epsilon$ ) of PA at 252 nm,  $6928 \text{ cm}^{-1}\cdot\text{M}^{-1}$ , which was used to estimate the DS.

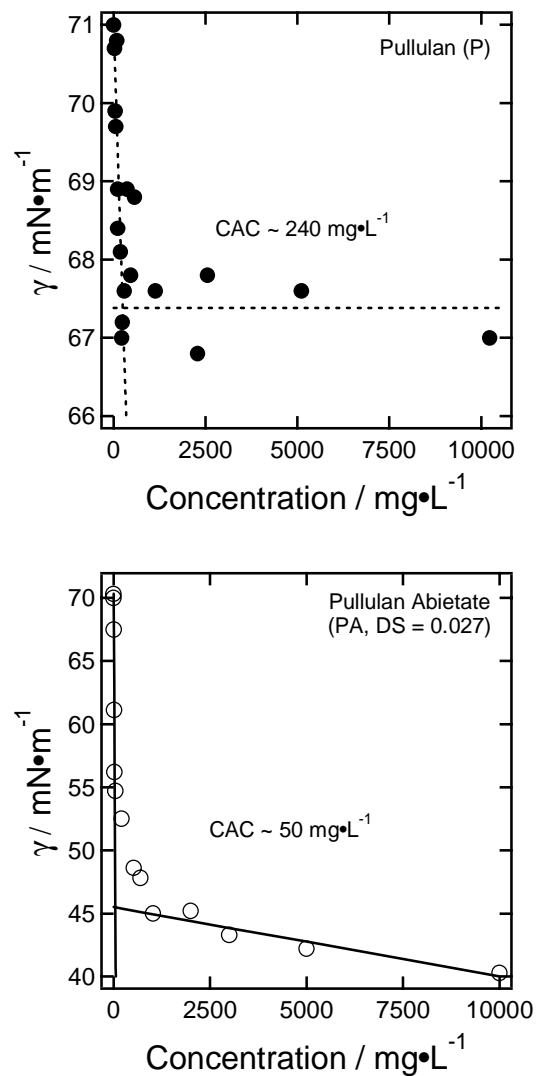


Figure 4. Determination of the critical aggregation concentration (cac) of P and PA using the Wilhelmy plate technique. The copolymer has a lower cac value,  $50 \pm 5$  vs.  $240 \pm 50$   $\text{mg/L}$ , indicating a greater tendency to self-aggregate. Error estimates represent  $\pm$  one standard deviation. In addition, the copolymer impacts the maximum surface tension change of the solution more significantly than the homopolysaccharide.

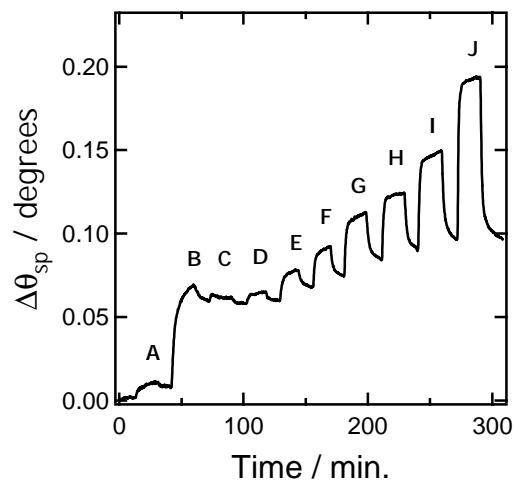


Figure 5. SPR results illustrating the adsorption and desorption process of PA at regenerated cellulose LB surfaces. The SPR sensor is alternately exposed to PA solutions (rise in  $\Delta\theta_{sp}$ ) and water (drop in  $\Delta\theta_{sp}$ ). The PA solution concentrations are A) 27, B) 56, C) 106, D) 212, E) 524, F) 1024, G) 2000, H) 3000, I) 5000, and J) 10000  $\text{mg}\cdot\text{L}^{-1}$ .

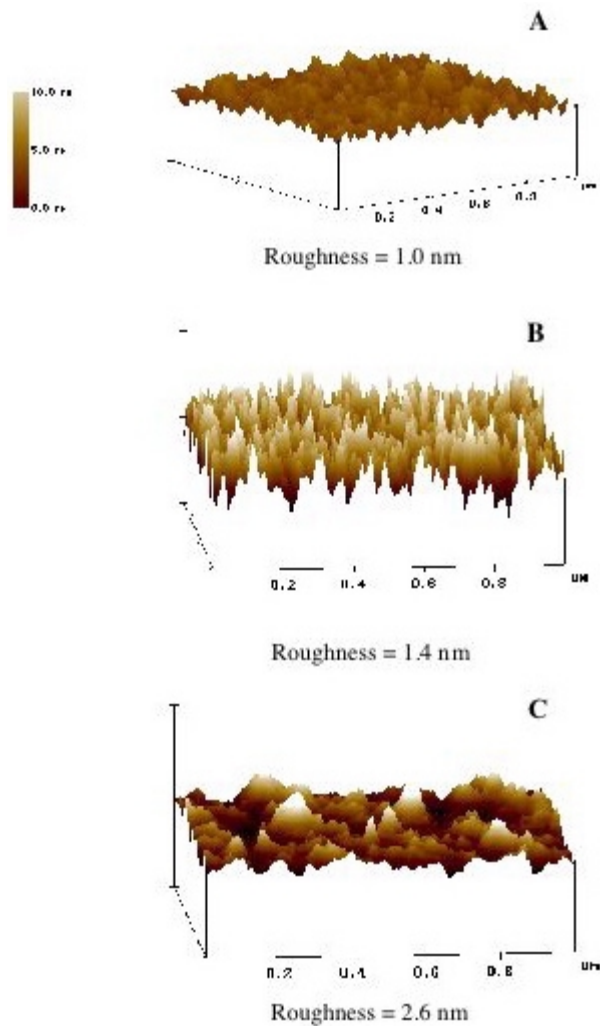


Figure 6. AFM images of cellulose LB-film surfaces before and after adsorption of P and PA: (A) regenerated cellulose before adsorption, (B) after adsorption of P, and (C) after adsorption of pullulan abietate. Note the change in the root mean square surface roughness, reflecting the modification of the surface by adsorption. All images are  $1 \mu\text{m} \times 1 \mu\text{m}$ .

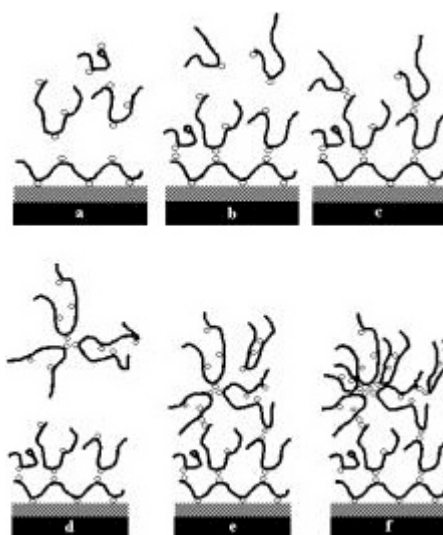


Figure 7. Illustration of the docking process of lignin-carbohydrate-like copolymers at cellulose surfaces. a-c demonstrates adsorption behavior below the cac, and d-f above the cac.